Electronic Supplementary Material (ESI) for Physical Chemistry Chemical Physics

Ultrafast photoinduced dynamics of halogenated cyclopentadienes: Observation of geminate charge-transfer complexes in solution

T. J. A. Wolf[a,*], O. Schalk[b,c], R. Radloff[a], G. Wu[b,d], P. Lang[c], A. Stolow[b], A.-N. Unterreiner[a,*]

Electronic Supplementary Information

1 ^{13}C-NMR characterization of C_5Br_6

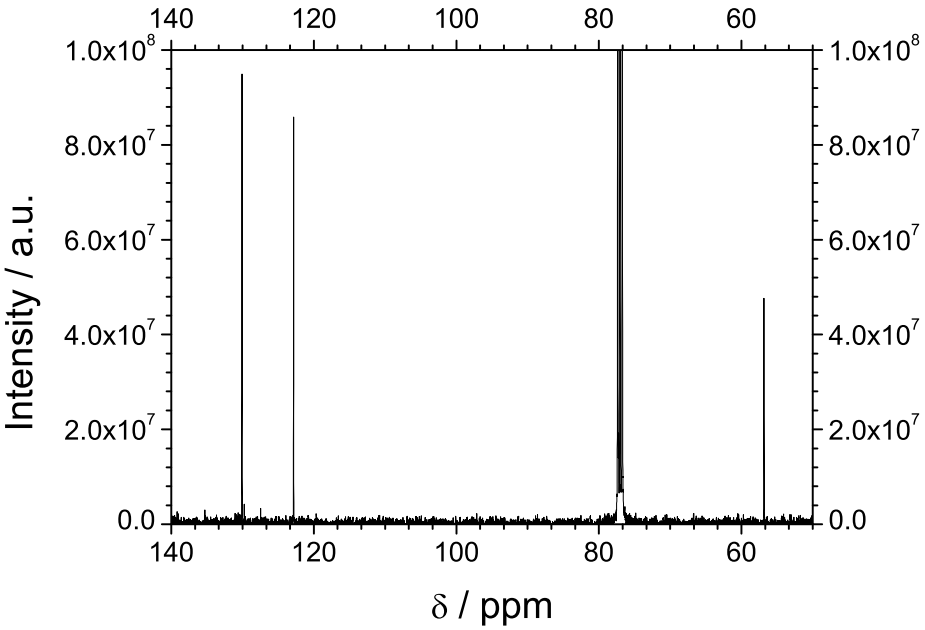

Figure †.1: ^{13}C-NMR spectrum of the synthesized C_5Br_6. The peaks at 77 ppm result from the solvent $CDCl_3$.

The ^{13}C-NMR spectrum of the synthesized C_5Br_6 is depicted in Fig. †.1. The peaks at 77 ppm originate from the employed solvent $CDCl_3$. The remaining peaks are in good agreement with literature-known spectra[1].

2 Spectra of C_5Cl_6 and C_5Br_6 in different solvents

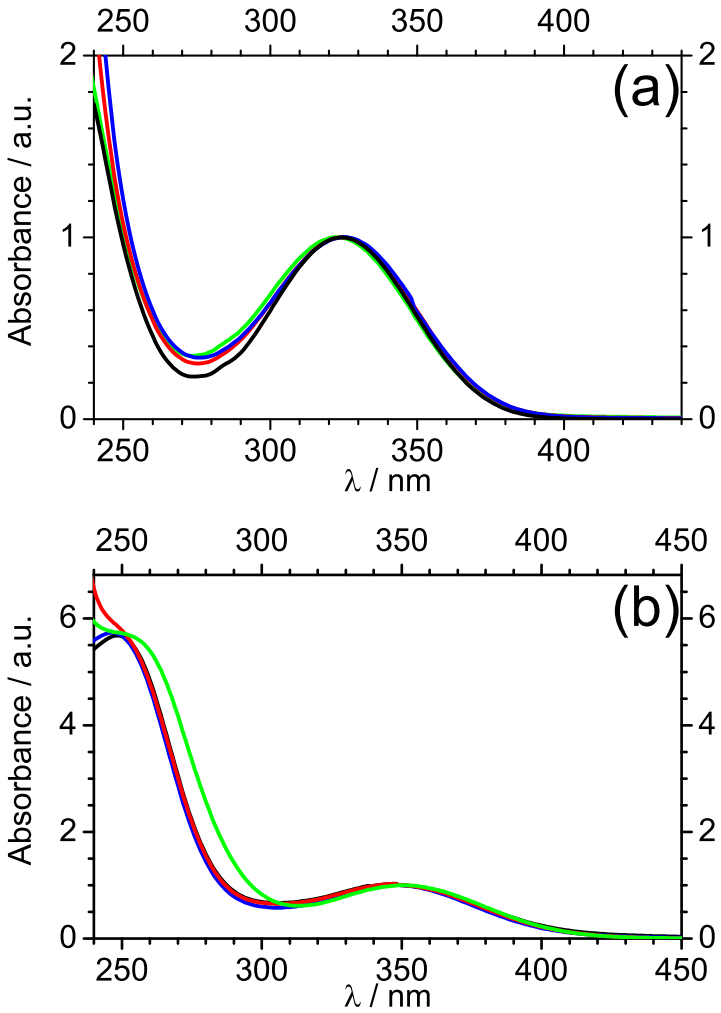

Figure †.2: Absorption spectra of (a) C_5Cl_6 and (b) C_5Br_6 in cyclohexane (black), isopropanol (blue), chloroform (red) and trichloroethanol (green). The spectra are normalized with respect to the extinction at (a) 323 nm and (b) 350 nm.

The spectra of C_5Cl_6 and C_5Br_6 in the employed solvents cyclohexane, isopropanol, chloroform and trichloroethanol are depicted in Fig. †.2 (a) and (b). The spectral shift of C_5Br_6 in trichloroethanol in Fig. †.2 (a) originates from a nonzero solvent absorption in the spectral region of the second absorption band.

3 Fit function for transient absorption traces

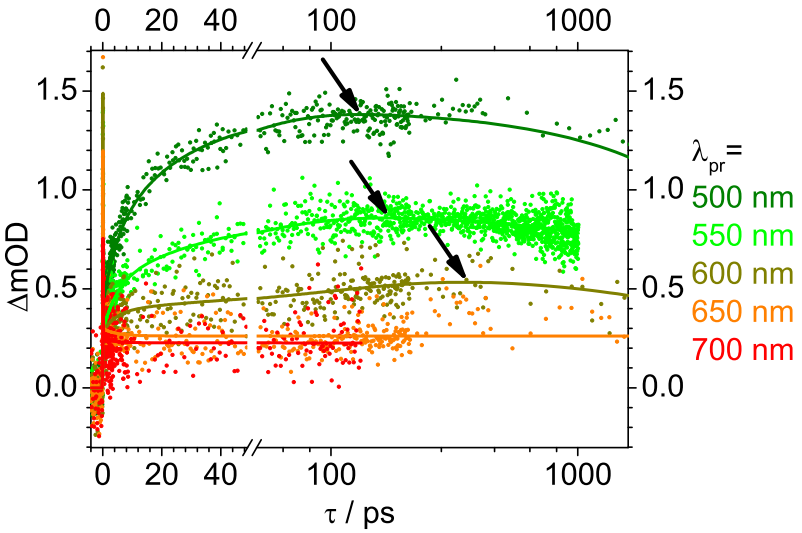

Figure †.3: Transient absorption traces (symbols) of C_5Br_6 in isopropanol and global fit analysis (lines). Molecules are excited at $\lambda_p = 350$ nm. The TA maximum shifts to longer delay times at longer λ_{pr} as indicated by the arrows.

All recorded TA traces in one specific solvent were globally fitted with functions of the type

$$\Delta OD(\lambda_{pr}, \tau) = g(\tau) \otimes \left(\sum_i A_i(\lambda_{pr}) \cdot P_i(\tau) \right). \quad (1)$$

The function represents a sum of i population or depopulation steps, each exhibiting a decay associated difference spectrum (DADS) $A(\lambda_{pr})$ and a time dependent population $P(\tau)$, which is expressed by exponential functions with time constants τ_i as parameters. The sum is convoluted with the instrument response function $g(\tau)$. For the fits $P(\tau)$ was set up as a 4-fold exponential function, where τ_1, τ_2, τ_3, and τ_4 were globally optimized for all TA traces in one solvent. For C_5Br_6 in isopropanol and trichloroethanol and for C_5Cl_6 in trichloroethanol τ_3 was optimized separately for each λ_{pr} to model the spectral shift in the TA maxima.

The resulting time constants are listed in Tab. 2 and 3 in the paper, respectively. Generally, multiexponential fits can be quite unstable and fit parameters correlated. The confidence intervals given for the time constants are, therefore, not extracted directly from the fitting procedure, but result from a comparison of the results of the global fit with results of individual fits of the TA traces.

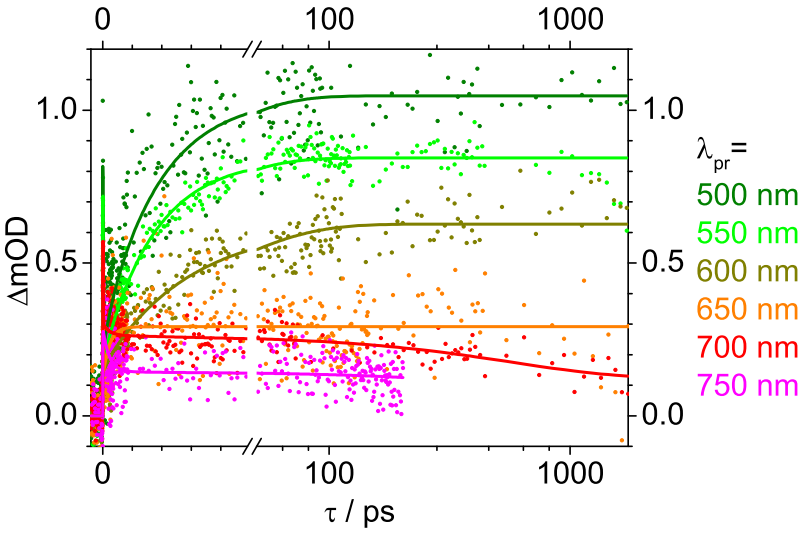

Figure †.4: Transient absorption traces (symbols) of C_5Br_6 in chloroform and global fit analysis (lines). Molecules are excited at $\lambda_p = 350$ nm.

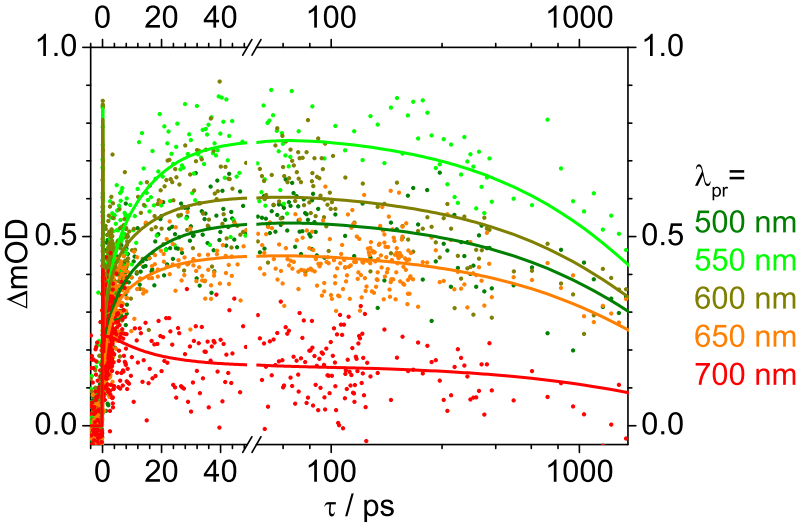

Figure †.5: Transient absorption traces (symbols) of C_5Cl_6 in chloroform and global fit analysis (lines). Molecules are excited at $\lambda_p = 323$ nm.

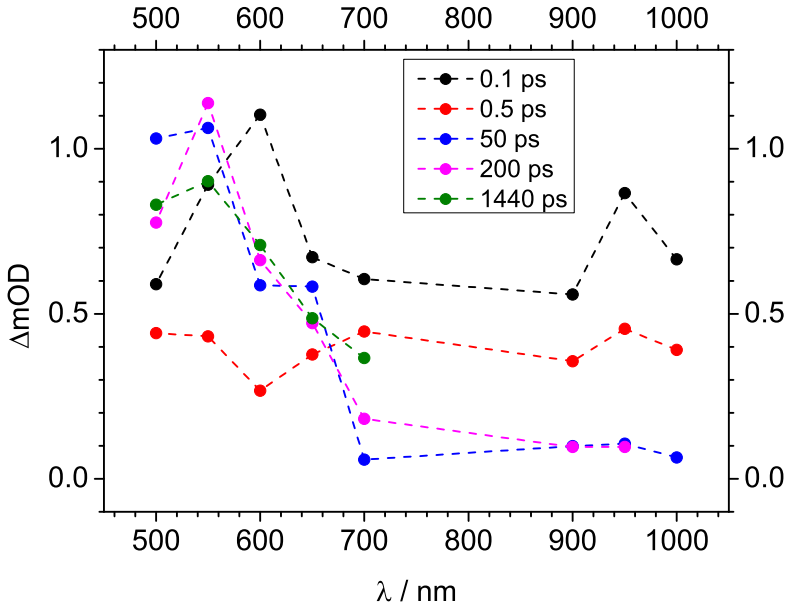

Figure †.6: Raw data transient spectra of C_5Br_6 in trichloroethanol at different pump-probe delay times constructed from the transient absorption traces, which are presented in Fig. 3 in the paper.

4 TRPES spectra of C_5Cl_6

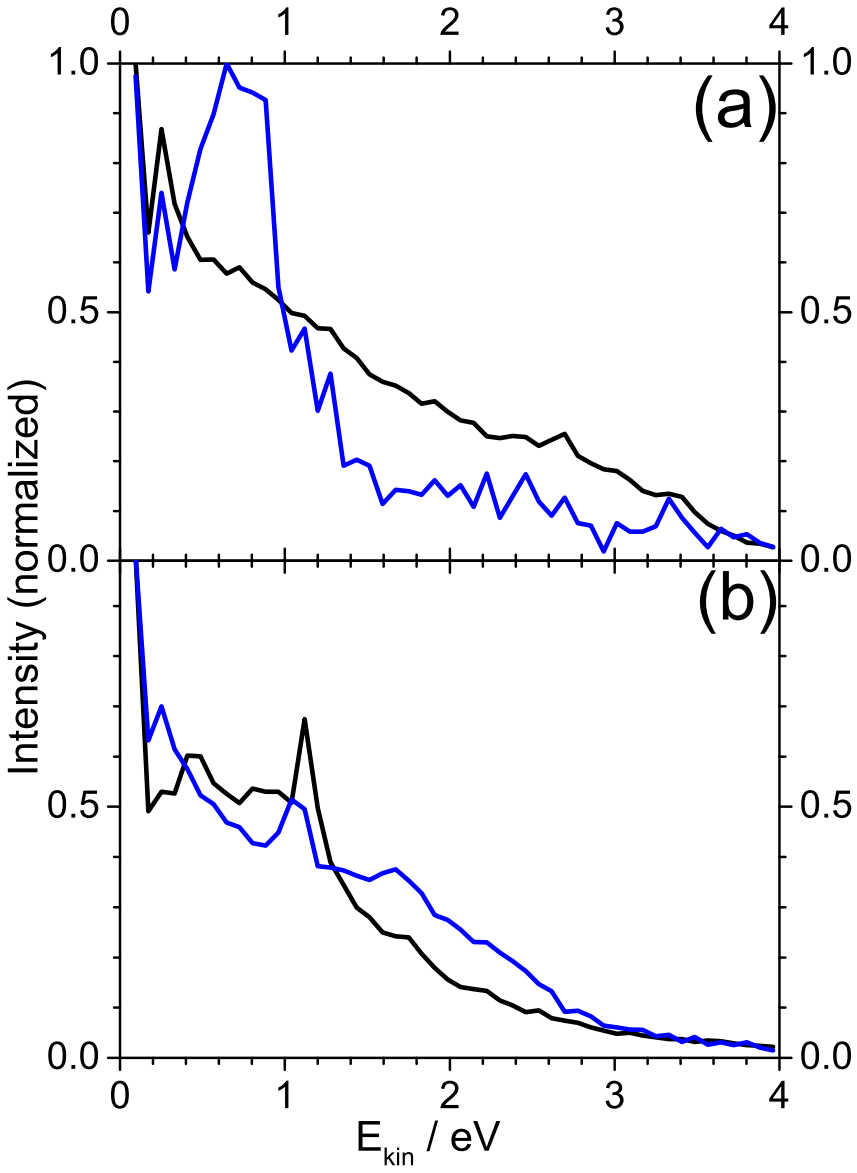

Figure †.7: Decay associated spectra of the time constants τ_1 (black) and τ_2 (blue) resulting from fits according to equation 2 of the C_5Cl_6 TRPES spectra at $\lambda_p = 315$ nm and (a) $\lambda_{pr} = 267$ nm and (b) $\lambda_{pr} = 400$ nm.

Neither a photoelectron spectrum nor an experimental ionization potential (IP) of C_5Cl_6 is known. However, the value of 8.89 eV, calculated with CCSD/def2-TZVP[2–6], is in good agreement with the maxima of the otherwise

broad and featureless one color photoelectron spectra of both λ_{pr}. An IP of 8.89 eV leads to a maximum kinetic energy of photoelectrons by ionization with one pump photon of 315 nm and two probe photons of 267 nm ([1,2'] ionization) of 4.34 eV. In the case of $\lambda_{pr} = 400$ nm the maximum kinetic energies are 1.26 eV and 4.34 eV for a [1,2'] and [1,3'] photon ionization, respectively. A slight growth in intensity can be observed for the stable photoelectron band at 400 nm ionization on the time scale of the experiment.

The TRPES spectra are cut into slices of $\Delta E \approx 0.08$ eV and fitted with a biexponential function of the type

$$S\left(E,\tau\right) = g(\tau) \otimes \left(\sum_i A_i(E) \cdot P_i(\tau) \right). \tag{2}$$

Here, A_i(E) represents the decay associated spectrum (DAS) of state i, $P_i(\tau)$ its time dependent population and g(τ) the instrument response function. For fitting the observed intensity growth on the 300 ps time scale in the TRPES spectrum at $\lambda_{pr} = 400$ nm an additional time constant $\tau_3 = 557$ ps is employed. As the intensity growth is not found at $\lambda_{pr} = 267$ nm, it is unlikely that these dynamics are connected to the investigated reaction dynamics on the femtosecond timescale. A convolution between τ_1 and τ_3 can be ruled out due to the high difference of the values. The values of the time constants τ_1 and τ_2 obtained by a Levenberg-Marquardt routine are listed in Tab. 4 in the paper. The confidence intervals given for the τ_1 values by the fitting routine are considerably smaller than the difference of the τ_1 values obtained from analysis of the two data sets of C_5Cl_6 at different λ_{pr}. Hence, the deviation of the values from their average is assumed instead as the error of the τ_1 values and also given in Tab. 4 in the manuscript. The DAS connected to the time constants τ_1 and τ_2 are depicted in Fig. †.7.

5 TRPES spectrum of C_5Br_6

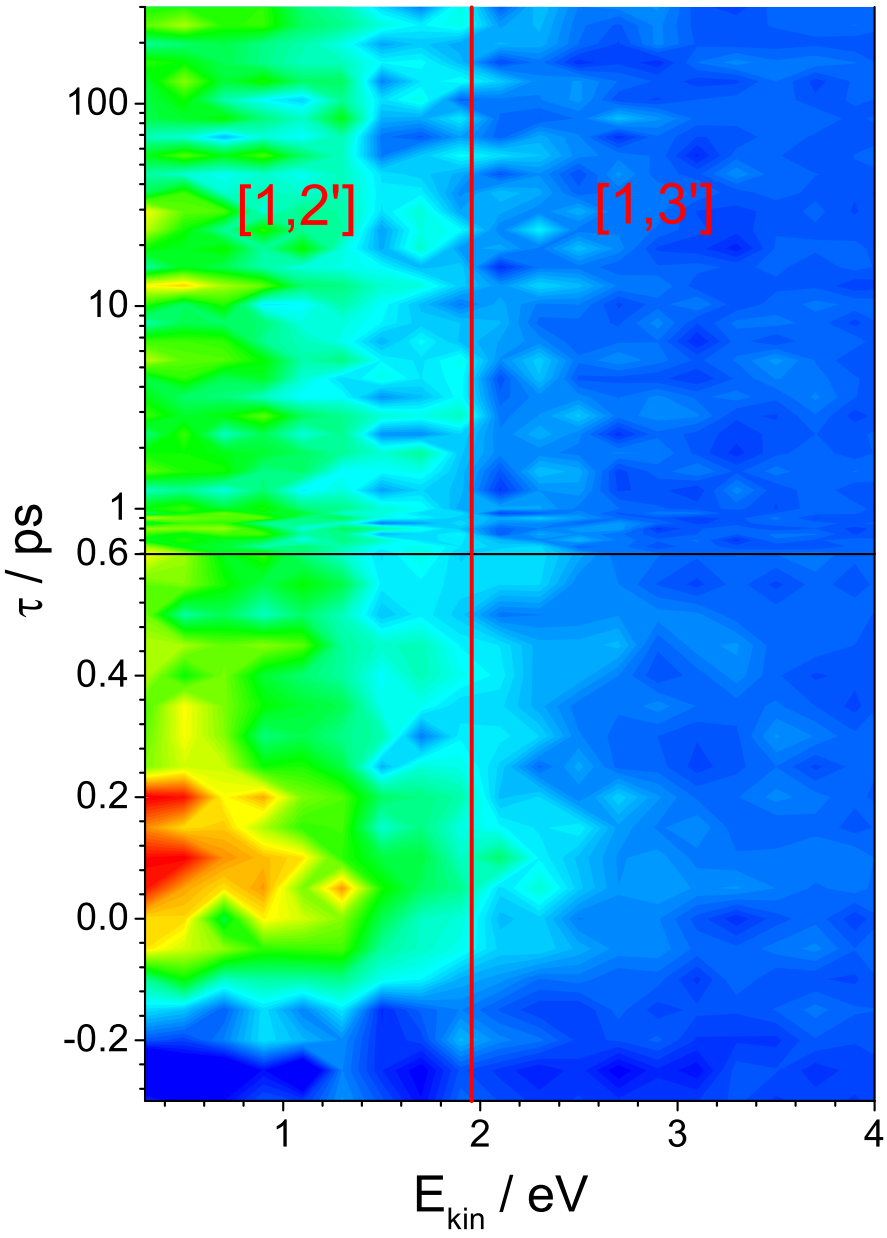

Figure †.8: Time resolved photoelectron spectrum of C_5Br_6 at $\lambda_p = 315$ nm and $\lambda_{pr} = 400$ nm. The energy cutoff between [1,2'] and [1,3'] photon ionization 1.96 eV is marked by a red line.

The TRPES spectrum of C_5Br_6 at $\lambda_p = 315$ nm and $\lambda_{pr} = 400$ nm is shown in Fig. †.8. Additionally, the cutoff between [1,2'] and [1,3'] photon ionization at 1.96 eV (based on an IP of 8.18 eV, calculated by B3LYP/def2-TZVP[5,7–11]) is

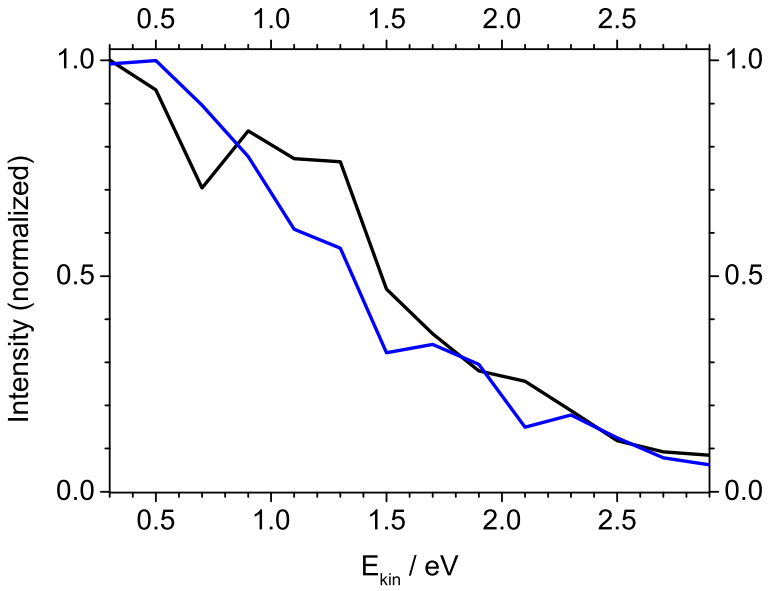

Figure †.9: Decay associated spectra of the processes associated with the time constants τ_1 (black) and τ_2 (blue), which result from fits according to equation 2 of the C_5Br_6 TRPES spectrum at $\lambda_p = 315$ nm and $\lambda_{pr} = 400$ nm.

marked. The spectrum shows a temporal and spectral behavior comparable to the TRPES spectra of C_5Cl_6. A component with broader spectral signature can be observed around $\tau = 0$. A second component is persistent on the investigated time scale. The TRPES spectrum is fitted according to Eq. 2. Time constants are listed in Tab. 4 in the paper and the decay associated spectra are depicted in Fig. †.9.

6 Estimation of the dissociation energies of the charge-transfer complexes

To ensure that the optimized charge-transfer complex minima are not an artifact due to a basis set superposition error, counterpoise correction calculations as implemented in Turbomole were performed with B3LYP/def2-TZVP. The counterpoise-corrected dissociation energies are calculated to be 28 kJ/mol ($C_5Cl_5\cdots Cl$) and 33 kJ/mol ($C_5Br_5\cdots Br$).

7 TDDFT calculation of C_5Cl_5 excitation energies

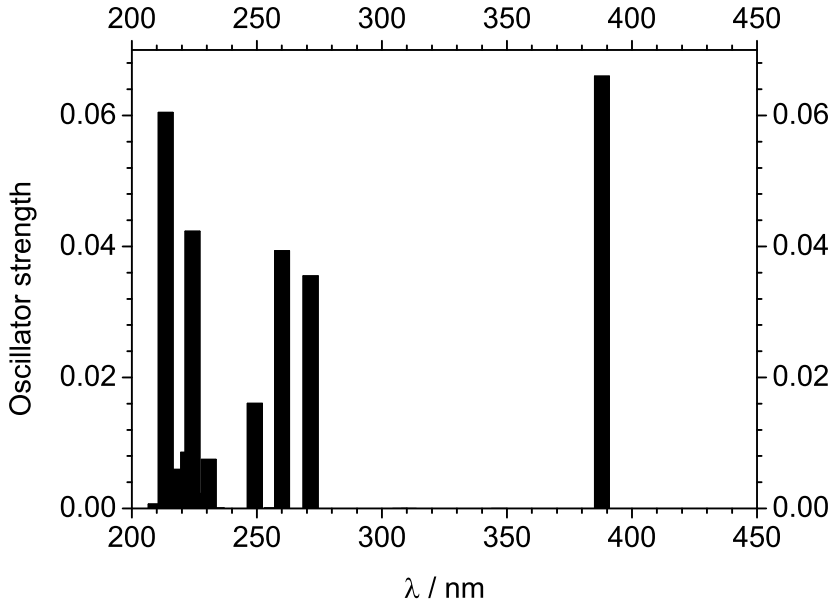

Figure †.10: Absorption spectrum of C_5Cl_5 calculated with TDDFT/B3LYP/ aug-cc-pVDZ. An additional excitation with zero oscillator strength is calculated to appear at $\lambda = 1614$ nm.

Electronic transitions from the ground state of the C_5Cl_5 radical calculated at the TDDFT/ B3LYP/aug-cc-pVDZ level of theory are shown in Fig. †.10. C_5Cl_5 is a Jahn-Teller system, which exhibits a degenerate ground state at D_{5h} symmetry and is therefore expected to show symmetry lowering to C_{2v} in the ground state resulting in a so-called umbrella potential for the two symmetry lowering normal modes. Nonetheless, EPR spectroscopy in solution gave hints for D_{5h} symmetry. The finding can be explained with the umbrella potential being shallow enough that the first vibrational state is higher in energy than the conical intersection at D_{5h} symmetry[12]. Naturally, any single reference method is questionable in the direct vicinity of a point of degeneracy. However, the

nearly degenerate electronic states are also found in the TDDFT calculation as a transition with zero oscillator strength at $\lambda = 1614$ nm. Additionally, the first intense transition is found at 400 nm as expected from experimental findings[12,13].

8 Interpolated paths

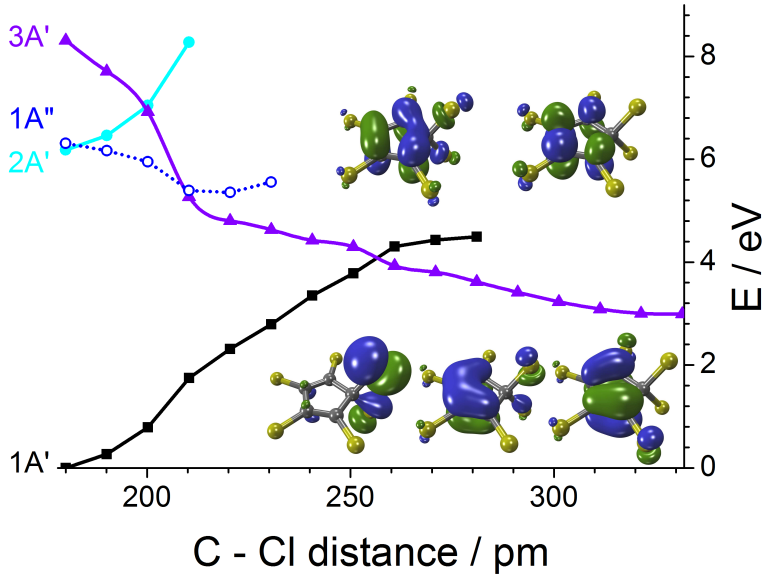

Figure †.11: Interpolated path between the C_5Cl_6 minimum geometry and the minimum geometry of the $C_5Cl\cdots Cl$ complex. The calculations were performed on the SA-4-CASSCF(6,5)/6-31G* level of theory. The abscissa resembles the C - Cl bond dissociation coordinate. States with A'-symmetry are labeled with solid lines, states with A"-symmetry with dotted lines. The numbering of the states is according to their energetical position at the Franck-Condon geometry. The 1A' (black), 1A" (blue) and 3A' (violet) have preferentially singly excited character, the 2A' (light blue) state exhibits considerable doubly excited character. Additionally, the molecular orbitals constituting the CAS are inserted. The MOs with A' symmetry are depicted in the first row, the MOs with A" symmetry in the second row.

To ensure that the results of CC2 calculations are not corrupted by the poor ability of CC2 to treat doubly excited states, we calculated an interpolated path at the same geometries employing SA-4-CASSCF(6,5) (see Fig. †.11). This method is able to describe the excited states qualitatively correct. The active space consists of the four π-MOs of C_5Cl_6 (see Fig. †.11), two of them with A' symmetry, the other two with A" symmetry. Additionally, an MO mainly consisting of two Cl p-AOs is included (Fig. †.11 first row, middle), since the 3 A' state predominantly corresponds to a single excitation from this MO.

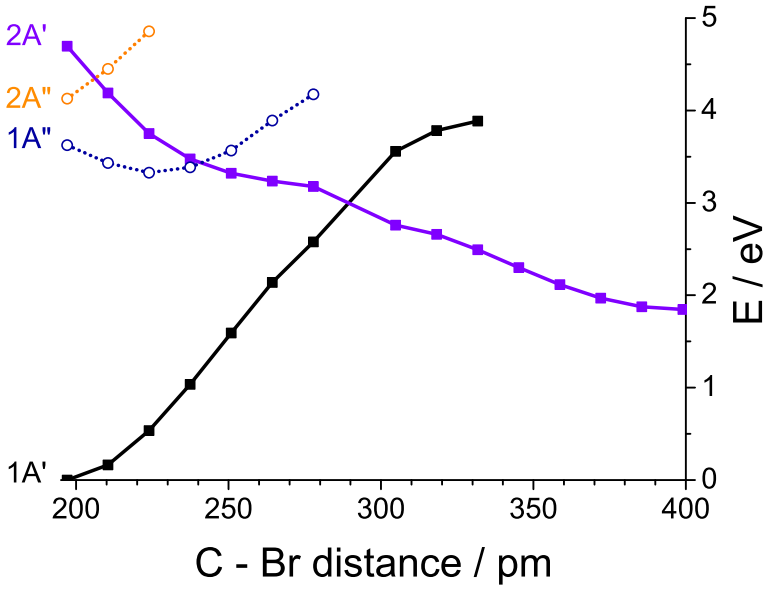

Figure †.12: Interpolated path between the C_5Br_6 minimum geometry and the minimum geometry of the $C_5Br\cdots Br$ complex. The calculations were performed on the CC2/aug-cc-pVDZ level of theory. The abscissa resembles the C - Cl bond dissociation coordinate. States with A' symmetry are labeled with solid lines, states with A" symmetry with dotted lines. The numbering of the states is according to their energetical position at the Franck-Condon geometry.

Additionally, an interpolated path analogue to C_5Cl_6 was calculated for C_5Br_6 on the CC2/aug-cc-pVDZ level of theory. The state, which is labeled as 3A' in the case of C_5Cl_6, is the first excited singlet state with A' symmetry (2A') in C_5Br_6.

References

[1] G. E. Hawkes, R. A. Smith and J. D. Roberts, *J. Org. Chem.*, 1974, **39**, 1276–1290.

[2] C. Hättig and F. Weigend, *J. Chem. Phys.*, 2000, **113**, 5154–5161.

[3] C. Hättig and A. Köhn, *J. Chem. Phys.*, 2002, **117**, 6939–6951.

[4] A. Köhn and C. Hättig, *J. Chem. Phys.*, 2003, **119**, 5021–5036.

[5] F. Weigend and R. Ahlrichs, *Phys. Chem. Chem. Phys.*, 2005, **7**, 3297–3305.

[6] A. Schafer, C. Huber and R. Ahlrichs, *J. Chem. Phys.*, 1994, **100**, 5829–5835.

[7] O. Treutler and R. Ahlrichs, *J. Chem. Phys.*, 1995, **102**, 346–354.

[8] K. Eichkorn, O. Treutler, H. Öhm, M. Häser and R. Ahlrichs, *Chem. Phys. Lett.*, 1995, **240**, 283–290.

[9] K. Eichkorn, O. Treutler, H. Öhm, M. Häser and R. Ahlrichs, *Chem. Phys. Lett.*, 1995, **242**, 652–660.

[10] F. Weigend, *Phys. Chem. Chem. Phys.*, 2006, **8**, 1057–1065.

[11] A. Schäfer, H. Horn and R. Ahlrichs, *J. Chem. Phys.*, 1992, **97**, 2571–2577.

[12] F. Graf and H. H. Günthard, *Chem. Phys. Lett.*, 1970, **7**, 25–28.

[13] F. Graf and H. H. Günthard, *Chem. Phys. Lett.*, 1971, **8**, 395–398.